Atmos. Chem. Phys. Discuss., 9, 635–671, 2009
www.atmos-chem-phys-discuss.net/9/635/2009/

Atmospheric Chemistry and Physics Discussions

This discussion paper is/has been under review for the journal *Atmospheric Chemistry and Physics (ACP)*. Please refer to the corresponding final paper in *ACP* if available.

Gas/particle partitioning of water-soluble organic aerosol in Atlanta

C. J. Hennigan[1], M. H. Bergin[1,2], A. G. Russell[1], A. Nenes[2,3], and R. J. Weber[2]

[1]School of Civil and Environmental Engineering, Georgia Institute of Technology, USA
[2]School of Earth and Atmospheric Sciences, Georgia Institute of Technology, USA
[3]School of Chemical and Biomolecular Engineering, Georgia Institute of Technology, USA

Received: 29 October 2008 – Accepted: 14 November 2008 – Published: 8 January 2009

Correspondence to: R. J. Weber (rweber@eas.gatech.edu)

Published by Copernicus Publications on behalf of the European Geosciences Union.

Abstract

Gas and particle-phase organic carbon compounds soluble in water (e.g., WSOC) were measured simultaneously in Atlanta throughout the summer of 2007 to investigate gas/particle partitioning of ambient secondary organic aerosol (SOA). Previous studies have established that, in the absence of biomass burning, particulate WSOC ($WSOC_p$) is mainly from secondary organic aerosol (SOA) production. Comparisons between $WSOC_p$, organic carbon (OC) and elemental carbon (EC) indicate that $WSOC_p$ was a nearly comprehensive measure of SOA in the Atlanta summertime. To study SOA formation mechanisms, WSOC gas-particle partitioning was investigated as a function of temperature, RH, NO_x, O_3, and organic aerosol mass concentration. Identifying a clear temperature effect on partitioning was confounded by other temperature-dependent processes, which likely included the emissions of biogenic SOA precursors and photochemical SOA formation. Relative humidity data indicated a linear dependence between partitioning and fine particle liquid water. Lower NO_x concentrations were associated with greater partitioning to particles, but WSOC partitioning had no visible relation to O_3 or fine particle OC mass concentration. There was, however, a relationship between WSOC partitioning and the $WSOC_p$ concentration, suggesting a compositional dependence between partitioning semi-volatile gases and the phase state of the aerosol. Combined, the overall results suggest that partitioning to liquid water, followed by heterogeneous reactions may represent the main process by which SOA is formed in urban Atlanta during summer.

1 Introduction

The gas/particle partitioning of oxidized semi-volatile organic compounds (SVOCs) is an integral process in the formation of secondary organic aerosol (SOA), making it one of the most important routes for producing fine atmospheric particles. At present, there is little data that characterizes the total gas/particle partitioning of ambient SOA, largely

ACPD
9, 635–671, 2009

due to the plethora of species involved in partitioning and the highly complex nature of SOA. Ambient studies have, however, examined the partitioning of individual secondary organic compounds. For example, Matsunaga et al. (2005) simultaneously measured ten carbonyls in the gas and particle phases at a site near Tokyo, while Fisseha et al. (2006) made simultaneous measurements of four carboxylic acids in the gas and particle phases in Zurich. One limitation to these studies, and others like them, is that they characterize a very minor fraction of the total SOA (and hence, organic carbon aerosol (OC)) mass, so their behavior may not be representative of the SOA. Additionally, heterogeneous reactions may alter the condensed phase component to forms difficult to detect, which would then not be considered in single component analysis partitioning studies.

Smog chamber experiments have described the gas/particle partitioning behavior of total SOA generated from a given volatile organic compound (VOC) or VOC mixture. Evidence from chamber experiments suggests that the partitioning of SVOCs between gas and particle phases is highly dependent upon the organic aerosol mass (Odum et al., 1996, 1997; Hoffmann et al., 1997), consistent with SOA gas/particle partitioning models (e.g., Pankow, 1994). The strong temperature dependence of SOA formation in smog chamber experiments is also consistent with partitioning theory (Takekawa et al., 2003). The translation of these studies to the ambient atmosphere remains a challenge, as current models employing these mechanisms systematically under-predict ambient SOA concentrations (de Gouw et al., 2005). The cause(s) of this discrepancy is still not clear, and is not necessarily the result of uncertainties in the partitioning model: other factors could be responsible, including additional SOA precursors not currently considered (Goldstein and Galbally, 2007; Volkamer et al., 2008). The lack of ambient data that may provide clear and comprehensive mechanistic insights into the SOA formation process inhibits an understanding of the exact causes for the modeling discrepancies.

In this study, we analyze the gas/particle partitioning of ambient SOA through extensive and highly time-resolved measurements of water-soluble organic carbon com-

pounds in the gas ($WSOC_g$) and particle ($WSOC_p$) phases in summertime Atlanta. In making a bulk measurement like WSOC, chemical specificity related to individual compounds is lost, but instead a major fraction of the SOA and hence, a large fraction of total OC mass is characterized.

2 Methods

Ambient gas and particle measurements were conducted from 11 May–20 September 2007 on the Georgia Institute of Technology Campus, located near the center of Atlanta. The measurement platform was ~30–40 m above ground, and the instruments were located in the rooftop laboratory of the Ford Environmental Science & Technology Building.

$WSOC_p$ measurements were conducted via a particle-into-liquid sampler (PILS) coupled to a Total Organic Carbon analyzer, a method which has been detailed by Sullivan et al. (2004). Briefly, particles with aerodynamic diameter less than 2.5 µm, selected using a non-rotating micro-orifice impactor (Marple et al., 1991), were collected into the liquid phase by a PILS (Orsini et al., 2003) operated at 15 L min^{-1}. The aqueous sample was then transferred to a Total Organic Carbon (TOC) analyzer (GE Analytical) for the semi-continuous determination of the water-soluble fraction of the carbonaceous aerosol. Two studies have shown that this approach agrees to within ~10% with $WSOC_p$ extracted from integrated filters (Sullivan and Weber, 2006; Miyazaki et al., 2006). The TOC analyzer was operated with a six-minute integration time, the maximum sampling rate of the analyzer employed. Twice daily, the sample airstream was diverted through a filter to determine the organic carbon content of the collection water and any interference from VOCs potentially collected by the PILS. This dynamic blank was subtracted from sample organic carbon values to quantify the ambient concentration of $WSOC_p$. The limit of detection was approximately 0.1 µg C m^{-3} and the estimated uncertainty of the method is ~10% (Sullivan et al., 2004).

$WSOC_g$ concentrations were measured with a method similar to that of Anderson et

al. (2008), but modified and configured for the present study. Sample air was pulled at 21±1 L min^{-1} though a Teflon filter for the complete removal of particles, and immediately entered a glass mist chamber (MC) (Cofer and Edahl, 1986) initially filled with 10 mL of ultra-pure (>18.0 MΩ, low carbon) water. The MC, which was operated with a sample residence time of approximately 0.45 s, efficiently collects gases with a Henry's Law constant greater than 10^3 M atm^{-1} (Spaulding et al., 2002). The collection efficiency was tested using nitric acid, and found to be 95.1%±2.1% (mean ±1σ). One five-minute batch sample was collected every ten minutes using an automated valve to open and close flow from the MC to the vacuum pump. Once collected, the sample was analyzed by a Total Organic Carbon analyzer (GE Analytical). In between sample analyses, the carbon content of the 18.0 MΩ ultra-pure water was determined and the MC was rinsed with the ultra-pure water as well. The carbon content of the pure water was subtracted from the organic carbon content of the subsequent sample to quantify the organic carbon of the captured ambient organic gases.

Factory calibrations were performed on the two TOC analyzers used to measure $WSOC_p$ and $WSOC_g$, and sucrose standards were also periodically run over the full range (50–2000 ppb C) of expected liquid concentrations to verify proper analyzer accuracy throughout the measurement period.

Accurate determination of the concentrations measured with the MC depends on an accurate measure of the volume of water used to collect the sample. Consequently, water evaporation effects during sample collection need to be accounted for. Calibrations of water evaporation were performed using gravimetric analysis on three separate days (n total=56). It was found that evaporation was approximately constant, regardless of ambient temperature and relative humidity (RH) conditions. During the calibrations, ambient temperature exhibited a range of 18.5–32.4°C while ambient RH exhibited a range of 23–66%. With an initial volume of 10 mL, the ending volume after five minutes of sampling was 8.75 mL±0.12 mL (1.4%) at the 95% confidence interval. Because the ambient temperature and RH conditions encountered during calibrations covered much of the range observed during sampling, the assumption of a constant

ending water volume is assumed to be valid throughout the study period. At an air flow rate of 21 L min^{-1} and a five-minute sample integration time, the LOD for the $WSOC_g$ measurement was 0.9 µg C m^{-3}. Based on uncertainties in the airflow (±5%), ending water volume (±1.4%), TOC analyzer uncertainty (±2%), and uncertainty in the TOC background concentration (±2%), the overall estimated uncertainty for the $WSOC_g$ measurement is 7%.

Measurements of aerosol organic carbon (OC) and elemental carbon (EC) were made with a Sunset Labs OCEC Field Analyzer (Sunset Laboratory Inc., Tigard, OR) in accordance with NIOSH method 5040 (NIOSH, 1996). The measurements consisted of a 45-min collection period followed by 15 min of analysis time. The data are not blank-corrected and may be systematically overestimated by about 0.5 µg C m^3 (Peltier et al., 2007). At a sampling time of 45 min, the method uncertainty is estimated at 20% (Peltier et al., 2007). NO_x data were taken from the Georgia Department of Natural Resources (DNR) Ambient Monitoring Network (http://www.georgiaepd.org/air/amp/) site co-located with the aerosol measurements discussed above, while O_3 data were taken from a Georgia DNR site approximately 5 km from the Georgia Institute of Technology campus.

Measurements were carried out for approximately 4.5 months, with intermittent periods for instrument maintenance/repair and calibrations, such that the total number of observations was equivalent to approximately 3 months of continuous sampling. As detailed above, the measurements were carried out at a high time resolution; six minutes for the $WSOC_p$ measurement, a five-minute $WSOC_g$ sample every 10 min, and hourly for the OC and EC measurements. The high time resolution and extended length of the measurements resulted in the collection of extensive data sets (n=19 049 for $WSOC_p$, n=12 298 for $WSOC_g$, n=1478 for OC and EC, the sample size for an averaged dataset corresponds to the instrument with lower sampling rate), that provided high statistical significance for the analyses performed. This not only enhances their significance, but may provide insights into overall trends that would not have been detected with a shorter data set due to the many short-term factors that cause day-to-day variability

in ambient SVOC and particle concentrations.

3 Results and discussion

3.1 WSOC in Atlanta

In the following analysis, infrequent periods of biomass burning influence were removed from the data set. For the entire summer, $WSOC_p$ was in the range of 0.2–12.1 $\mu g\,C\,m^{-3}$ and had an average concentration of $3.3 \pm 1.8\,\mu g\,C\,m^{-3}$ (mean $\pm 1\sigma$, for n=19 049). $WSOC_p$ was highly correlated with OC (R^2=0.73) and the slope (0.70 $\mu g\,C/\mu g\,C$) indicates that a high fraction of the OC was soluble and hence likely to be secondary. (Note, the results are based on a Deming linear regression that minimizes the distance between the observed data and fitted line in both the x- and y-directions and is more appropriate than regular linear regression for this type of data (Cornbleet and Gochman, 1979)). The range of $WSOC_g$ concentrations observed for the entire summer was 1.1–73.1 $\mu g\,C\,m^{-3}$, and the mean $WSOC_g$ concentration was 13.7 $\mu g\,C\,m^{-3}$. Overall, $WSOC_p$ and $WSOC_g$ were correlated during the summer, though there was a large amount of scatter in the data (Fig. 1). A Deming linear regression gives a slope of 0.242 and an intercept of 0.266 $\mu g\,C\,m^{-3}$, as shown in the $WSOC_p$ vs. $WSOC_g$ plot of Fig. 1.

Since $WSOC_p$ and $WSOC_g$ have oxygenated functional groups, it is expected that both are mostly secondary. In Atlanta, particle and gas-phase WSOC predominantly originate from biogenic VOCs oxidation, since they dominate the VOC emissions budget (Environmental Protection Agency, National Emissions Inventory; Guenther et al., 1994). The correlation between $WSOC_p$ and $WSOC_g$ (Fig. 1) strongly supports a common source (biogenic VOCs). The large amount of scatter in the data, however, may indicate differences that include their formation mechanisms and atmospheric lifetimes.

The average diurnal trends of $WSOC_p$ and $WSOC_g$ are shown in Fig. 2. $WSOC_p$

ACPD
9, 635–671, 2009

reached an average daily maximum of 3.8 µg C m^{-3} at 14:00 (Eastern Daylight Time). On average, WSOC$_p$ steadily increased in concentration from a morning minimum of 3.1 µg C m^{-3} at 06:00 to a daily maximum of 3.8 µg C m^{-3} at 14:00. Following the afternoon concentration maximum, the average WSOC$_p$ concentration decreased until it reached a level of 3.2 µg C m^{-3} at 20:00. During the evening and night (between 20:00 and 06:00 the next morning) the median WSOC$_p$ concentration was relatively constant, ranging between 3.1–3.3 µg C m^{-3}. Between the hours of 06:00 and 20:00, diurnal profiles of WSOC$_p$ and WSOC$_g$ were highly similar. The average WSOC$_g$ peak concentration also occurred at 14:00 (14.5 µg C m^{-3}) in between minima at 06:00 (12.4 µg C m^{-3}) and 19:00 (12.3 µg C m^{-3}). The mid-day increases in WSOC$_p$ and WSOC$_g$ concentrations suggest photochemical formation, but the relatively modest enhancement (~20%) over pre-sunrise concentrations also suggests a substantial regional WSOC background and a relatively long lifetime of both classes of material. This is consistent with the findings of Weber et al. (2007), who showed the highly regional nature of WSOC$_p$ in and around Atlanta.

Unlike WSOC$_p$, the WSOC$_g$ concentration increased at night and had another maximum (15.4 µg C m^{-3}) at 23:00 that may result from monoterpene emissions from pine species, which can be maximum in the middle of the night (e.g., Simon et al., 1994; Hakola et al., 2000; Janson et al., 2001). This difference led to a lower WSOC$_p$/WSOC$_g$ slope at night (0.224) than during the day (0.260). Smog chamber experiments have demonstrated SOA formation from monoterpenes in the absence of UV from reactions initiated by ozone (i.e., ozonolysis reactions) (e.g., Hoffmann et al., 1997) and the nitrate radical (NO_3) (e.g., Griffin et al., 1999). Since monoterpenes are not soluble in water (Sander, 1999), the midnight peak in WSOC$_g$ suggests oxidative reactions were occurring at night, however, the lack of a nighttime peak in the median WSOC$_p$ concentration suggests that these oxidation reactions generally did not produce appreciable organic aerosol. Smog chamber studies by Hallquist et al. (1999) observed significantly lower SOA yields from the reactions of NO_3 with α-pinene, compared to

reactions of NO_3 with either β-pinene, Δ^3-carene, or limonene. Additionally, nighttime chamber studies by Griffin et al. (1999) observed significantly lower SOA yields from the ozonolysis of β-pinene than either the ozonolysis of α-pinene or the photooxidation of β-pinene. All of this suggests that a nighttime source and reaction mechanism(s) that produces $WSOC_g$, yet little $WSOC_p$, is plausible.

There is evidence that, in the absence of significant biomass burning influence, the compounds that make up $WSOC_p$ are largely secondary (Sullivan et al., 2006; Weber et al., 2007), although $WSOC_p$ may not be a completely comprehensive measurement of SOA in certain locations. For example, SOA estimated by the EC tracer method in Tokyo was highly correlated with $WSOC_p$ (R^2=0.70–0.79) and observed $WSOC_p$/SOA slopes were 0.67–0.75 (Miyazaki et al., 2006). The same study also found 90% or more of primary organic aerosol to be insoluble in water. A study by Favez et al. (2008) observed prominent formation of water-insoluble SOA in Cairo, a highly arid urban center. In Atlanta however, $WSOC_p$ is accounting for most, if not all, of the SOA. This can be seen from Fig. 3, where strong similarities between the mean diurnal profiles of water-insoluble organic carbon ($WIOC_p$=OC−$WSCO_p$) and elemental carbon (EC) are evident, indicating that it is mostly primary. Clear differences between the diurnal trends of $WIOC_p$ and $WSOC_p$ indicate very different sources between the two. Many studies have established that organic compounds constitute one of the largest fractions of $PM_{2.5}$ in Atlanta (e.g., Weber et al., 2003; Chu et al., 2004), thus at ~70% (gC/gC) of the summertime OC, processes contributing to $WSOC_p$ (i.e., SOA) have a large impact on the region's air quality.

3.2 WSOC partitioning

The fraction of total WSOC in the particle phase, F_p, is used to investigate partitioning, by,

$$F_p = \frac{WSOC_p}{WSOC_p + WSOC_g}. \quad (1)$$

F_p is related to the $WSOC_p/WSOC_g$ concentration ratio:

$$f_p = \frac{WSOC_p}{WSOC_g} = \frac{F_p}{1 - F_p}. \quad (2)$$

Various factors that may influence F_p are investigated in the following sections.

3.2.1 The F_p-temperature relationship

According to equilibrium gas/particle partitioning theory, temperature (T) imparts a strong effect on the gas/particle partitioning of organic compounds (Pankow and Bidleman, 1991). From Pankow (1994), an expression for the partitioning constant, K_p, is

$$K_p = \frac{C_p/M_o}{C_g} = \frac{760RTf_{om}}{10^6 MW_{om}\zeta p_i^\circ} \quad (3)$$

where K_p has units of $m^3\,\mu g^{-1}$, C_p is the compound's particle-phase concentration, M_o is the mass concentration of the absorbing organic phase (including water), and C_g is the compound's gas-phase concentration. K_p can also be predicted from the properties of the partitioning species, where R is the ideal gas constant, T is temperature, f_{om} is the organic fraction of total particulate mass, MW_{om} is the average molecular weight of the absorbing organic (and aqueous) phase, ζ is the particle-phase activity coefficient, and p_i° is the saturation vapor pressure. The vapor pressures of organic compounds approximately double for every 10 K temperature increase (Seinfeld et al., 2001). Thus, the temperature effect on partitioning in the ambient atmosphere will be dominated by the temperature effect on individual compound saturation vapor pressures, with higher temperature favoring the gas-phase and lower temperature favoring the particle phase. A strong temperature effect on SOA formation was observed in chamber studies using anthropogenic (toluene, m-xylene, 1,2,4-trimethylbenzene) and biogenic (α-pinene) VOCs (Takekawa et al., 2003).

For our ambient measurements, the box plot of Fig. 4 shows that there was no well-defined relationship between F_p and temperature (for median F_p vs. T, R^2=0.02), (also no relationship between f_p and temperature). The ambient temperature range was large enough (greater than 20°C) that any effect of temperature on WSOC partitioning should be present. It is likely, however, that a discernable temperature effect on partitioning was obscured by other temperature-dependent processes affecting WSOC and its precursor emissions.

Overall, median concentrations of both $WSOC_p$ (R^2=0.91) and $WSOC_g$ (R^2=0.97) were highly correlated with temperature (Fig. 5a and b). Thus, the central tendency over the entire summer was for higher WSOC concentrations to be associated with higher temperatures. The high correlation with median concentrations accompanied with a large amount of scatter in the overall data (evident from the spread in 10th, 25th, 75th, and 90th percentile values in Fig. 5) implicates temperature as one of multiple factors that affected WSOC concentrations. The emissions of biogenic precursors to WSOC (Tingey et al., 1980) and the photochemical formation of WSOC (Tsigaridis et al., 2005) are both positively related to temperature, and likely explain these trends. This suggests that the positive effects of temperature on biogenic emissions and reactivity may dominate over the negative effect of volatility on $WSOC_p$, demonstrated by the increase in both $WSOC_g$ and $WSOC_p$ with temperature.

It is possible that a temperature effect on WSOC gas/particle partitioning did exist, but was not visible due to the relationships $WSOC_p$ and $WSOC_g$ exhibited with temperature (Fig. 5a and b). The slopes of the median $WSOC_p$–T and the median $WSOC_g$–T correlation lines were 0.199 $\mu g\,C/m^3/°C$ and 0.821 $\mu g\,C/m^3/°C$, respectively. If background concentrations of $WSOC_p$ and $WSOC_g$ are both assumed zero, then, using the median relationships, a nominal temperature change would produce a constant F_p value of 0.195, which compares closely with the mean F_p for the entire study (0.203). This supports the view that a temperature-partitioning effect was obscured and highlights the dynamic nature of the ambient system in which the measurements were made. Specifically, an increase in temperature led to additional inputs of WSOC (parti-

ACPD
9, 635–671, 2009

cle and gas) into the system that made a determination of a specific temperature effect on partitioning ambiguous. This difficulty with ambient sampling underscores the need to pair ambient measurements with controlled laboratory experiments that can isolate experimental variables.

3.2.2 The F_p-RH and liquid water relationship

Hennigan et al. (2008a) observed, at RH levels >70%, a strong increase in F_p with RH that was likely due to liquid water uptake by fine ($PM_{2.5}$) particles. This is evident from the similarities between the F_p-RH curve and the two other independent predictions of liquid water uptake as a function of RH (Fig. 6). The RH effect on gas/particle partitioning led to increases in SOA mass (0.3–0.9 $\mu g\,C\,m^{-3}$) that were significant in the context of ambient concentrations. Figure 6 indicates a positive linear relationship between F_p and liquid water concentration (linear regression R^2 correlation between median F_p and liquid water for RH>45% is 0.997, n=5). Additionally, f_p ($WSOC_p/WSOC_g$, Eq. 2) also has a linear correlation coefficient (R^2) of 0.997 for RH>45%. Although these results point to a Henry's Law-type partitioning process (by Henry's Law the ratio of particle to gas concentration is directly proportional to liquid water concentration), we have noted that Henry's Law partitioning alone cannot account for the significant increase in F_p observed at elevated RH levels (Hennigan et al., 2008a). Additionally, application of Henry's Law assumes dissolution into an ideal solution, while ambient particles are non-ideal. The liquid water increase, even in a polluted atmosphere under high RH (>90%), is not enough to simply dissolve soluble semi-volatile gases (e.g., acetic acid or formic acid, etc.) and account for the SOA increase (Hennigan et al., 2008a).

Seinfeld et al. (2001) predict a substantial influence of liquid water on SOA formation due to the effect of water uptake on two terms in Eq. (3), MW_{om} and ζ. Though the effects of MW_{om} and ζ due to water uptake may be in competition, depending on the hydrophilic nature of the partitioning SVOCs, Seinfeld et al. (2001) predicted overall higher K_p values (more partitioning to the particle phase) at higher liquid water levels.

Pun and Seigneur (2007) also predict an enhancing effect of aerosol water on SOA formation due to the greater absorptive capacity of added water (the role in M_o, Eq. 3), its decreasing effect on the MW_{om} term (thus increasing K_p), and acid-catalyzed oligomer formation in the aqueous phase from glyoxal. Chang and Pankow (2008) propose an SOA model that incorporates the effects of water on MW_{om} and ζ, as shown by Seinfeld et al. (2001), while also including phase separation considerations.

Experimentally, the effect of water on SOA is not always present. Smog chamber studies by Cocker et al. (2001a, b) found no enhancement in SOA formation from α-pinene, m-xylene, or 1,3,5-trimethylbenzene due to liquid water. Edney et al. (2000) also found no water effect on SOA formation in smog chamber studies with toluene as the precursor VOC. In contrast, Volkamer et al. (2008) observed a positive linear dependence between acetylene (C_2H_2) SOA yields and the liquid water content of particles in chamber experiments. This was attributed to the gas phase hydroxyl radical (OH) oxidation of C_2H_2 to produce glyoxal and its subsequent uptake and reaction in the aqueous phase. Our ambient results showed a strong effect of RH on F_p, a linear relationship to particle liquid water, and so are in better agreement with the smog chamber results of Volkamer et al. (2008) and less-so with the traditional partitioning theory involving K_p.

3.2.3 The F_p-NO_x relationship

In addition to relative humidity, the data demonstrate that NO_x concentrations impacted F_p as well. A box plot of F_p verse RH was constructed after sorting the data according to NO_x concentrations, and mean values are plotted for the high NO_x and low NO_x data (Fig. 7a). The mean NO_x concentration for the high NO_x data was 33±23 ppb (mean $\pm 1\sigma$) while that for the low NO_x data was 6±2 ppb (mean $\pm 1\sigma$). Below 80% RH, low NO_x conditions were associated with higher values of F_p (mean=0.208), while high NO_x conditions were associated with lower values of F_p (mean=0.180). Overall, the mean F_p difference (0.028) below 80% RH was statistically significant at the 99.9% confidence interval (t=7.793 from student's t-test, df=1046). Multiplying this ΔF_p by

the mean total WSOC concentration below 80% RH (18.58 µg C m^{-3}) yields a $WSOC_p$ enhancement from this difference of 0.52 µg C m^{-3}. The difference in F_p values between high NO_x and low NO_x regimes (0.028) may appear small, despite its statistical significance. However, the difference is non-negligible given that the mean $WSOC_p$ concentration for the entire summer was 3.3 µg C m^{-3}.

The difference in WSOC partitioning with NO_x concentrations could explain the F_p differences observed between the nighttime and the daytime, where generally more WSOC was partitioned in the particle phase during the day than at night (Hennigan et al., 2008a). Though it is possible that the day/night differences in F_p were not driven by changes in NO_x concentrations, the evidence for a NO_x effect is compelling. Median F_p values had a strong negative linear correlation (r=−0.97) to NO_x concentrations (Fig. 7b). (Note, correlation remains strong (R=−0.84) even with the highest NO_x point removed). The data was also subdivided into day/night periods to investigate the role of NO_x during these times. When only daytime data was considered, the mean F_p value corresponding to the top 15% of NO_x concentrations was statistically lower (at the 99.5% confidence level) than the mean F_p value for the bottom 15% of NO_x concentrations (t=3.111 from student's t-test, df=264). This was also the case for nighttime only data (t=4.676 from student's t-test, df=335) and it supports the existence of a NO_x effect on F_p versus an indirect impact from another effect, such as oxidant (OH, O_3) concentration.

In general, SOA yields from the reaction of hydrocarbons with ten or fewer carbon atoms are significantly higher at low NO_x concentrations compared to high NO_x concentrations (Kroll and Seinfeld, 2008). These small hydrocarbons include isoprene (Kroll et al., 2006; Pandis et al., 1991) and monoterpenes (Presto et al., 2005; Ng et al., 2007), biogenic species with high emission rates in the Southeast (Guenther et al., 1994). Conversely, SOA yields from the reaction of larger hydrocarbons are, in general, highest at high NO_x levels (Kroll and Seinfeld, 2008). The NO_x effect on SOA yields arises from its substantial influence on the oxidant initiating SOA formation (i.e., hydroxyl radical, nitrate radical, or ozone) and on the fate of the RO_2 and RO radi-

cals (Kroll and Seinfeld, 2008). In general, reaction of smaller VOCs in the presence of higher NO_x concentrations leads to the formation of higher volatility products (e.g., fragmentation and formation of short aldehydes) compared to smaller VOC reactions in low NO_x conditions that produce lower volatility products (e.g., hydroperoxides and acids from reaction of RO_2+HO_2). As isoprene and monoterpenes are expected to be the major SOA precursors in the southeastern US, the observed relationship between F_p and NO_x is qualitatively consistent with the smog chamber studies which observed a similar phenomenon.

A limitation with the non-chemically specific approach used here is that F_p can depend on both the oxidation process leading to SVOCs and partitioning, similar to the process described by the Yield (Seinfeld and Pandis, 1998). Thus, this data does not provide evidence whether the observed NO_x effect is due to the types of SVOCs produced under different NO_x concentrations, or if NO_x plays a role in partitioning. Given the smog chamber results, the NO_x effect on the SVOCs product distribution seems the most likely cause for the observed effect on F_p.

In contrast to NO_x, ozone (O_3) concentrations did not appear to impact WSOC partitioning at all. The mean F_p at O_3 concentrations above 70 ppb (0.211) was not statistically different from the mean F_p at O_3 concentrations below 20 ppb (0.214). This result is in contrast to high aerosol yields from O_3 reactions with biogenic VOCs that have been observed in smog chamber studies (e.g., Griffin et al., 1999). It is possible, though, that O_3 was prominently involved in VOC oxidation but that O_3 was abundant, and VOCs limiting, in O_3-VOC reactions and thus little dependence was seen between F_p and O_3.

3.2.4 The F_p-organic aerosol mass relationship

Equation (3), along with extensive chamber experimental results (Odum et al., 1996, 1997; Hoffmann et al., 1997), suggests that the mass concentration of the absorbing organic phase, M_o, will also impact equilibrium gas/particle partitioning. The relationship suggests that, at a given temperature, a higher M_o will lead to a higher fraction

of a partitioning compound in the particle phase due to a greater capacity (i.e., surface area or volume) of absorbing medium for the partitioning of SVOCs. Figure 8a shows a box plot of F_p verse the organic carbon aerosol (OC) mass concentration and suggests that an F_p–M_o (i.e., F_p-OC) relationship did not exist over the entire summer. The total OC concentration was used because of

1. the strong dependence of SOA yields and partitioning on the total concentration (by mass) of organic aerosol in smog chamber studies (Odum et al., 1996), and

2. the substantial predictive capabilities of this method when used for subsequent smog chamber experiments of SOA formation from complex VOC mixtures (Odum et al., 1997).

For these reasons, this formulation has been widely applied to air quality models, but these data suggest this may not be appropriate in all environments.

Following the traditional line of reasoning on SOA formation, because F_p describes the partitioning of only water-soluble carbon compounds, $WSOC_p$ may be a more appropriate partitioning medium than OC due to the higher chemical similarities between $WSOC_p$ and $WSOC_g$ compared to similarities between OC and $WSOC_g$. This greater similarity arises because $WSOC_p$, and presumably $WSOC_g$, are predominantly secondary, while OC is comprised of significant fractions of both secondary and primary components. Alternatively, heterogeneous reactions involving $WSOC_p$ would also be expected to make investigating F_p relative to $WSOC_p$ a more appropriate parameter than OC.

Using $WSOC_p$ concentrations as the mass of the absorbing organic phase, the plot of F_p verses $WSOC_p$ (Fig. 8b) does suggest a relationship between gas/particle partitioning and existing organic aerosol mass. However, a dependence is only seen for $WSOC_p$ concentrations below $\sim 4\,\mu g\,C\,m^{-3}$. Higher $WSOC_p$ concentrations are associated with a larger fraction of total WSOC partitioned in the particle phase. This dependence between F_p and $WSOC_p$ appears to diminish and end at $WSOC_p$ above $\sim 4\,\mu g\,C\,m^{-3}$.

Though F_p and $WSOC_p$ are related (Eq. 1), we feel it is unlikely that the behavior of Fig. 8b was an artifact of the F_p-$WSOC_p$ dependence since the magnitude of $WSOC_g$ is significantly larger than $WSOC_p$, weakening any F_p-$WSOC_p$ direct dependence. Additional analyses support this view, and suggest that WSOC partitioning was impacted by the $WSOC_p$ concentration. (A number of tests were undertaken, including applying the Deming regression results of Fig. 1 to predict F_p, and testing randomly generated lognormal distributions of $WSOC_p$ and $WSOC_g$ based on observed medians and geometric standard deviations. Neither test resulted in an F_p-$WSOC_p$ dependence similar to the observations of Fig. 8b. Furthermore, plotting F_p vs. $WSOC_p$ is directly analogous to the plots of SOA Yield vs. M_o (e.g., Odum et al., 1996) used to formulate current partitioning theory).

An F_p dependence on $WSOC_p$ was also evident when the $WSOC_p$ concentration was incorporated into the F_p-RH analysis. Figure 9a shows that when the data were sorted according to $WSOC_p$ concentrations, there was a substantial difference in mean F_p values plotted against RH for high $WSOC_p$ concentrations (top 35% of data, mean $WSOC_p$=5.3 $\mu g\,C\,m^{-3}$) compared with low $WSOC_p$ concentrations (bottom 35% of data, mean $WSOC_p$=1.7 $\mu g\,C\,m^{-3}$). All of the eight points plotted were statistically different at the 99.9% confidence interval. Note that this high verse low $WSOC_p$ range spans the transition at ~4 $\mu g\,C\,m^{-3}$ in Fig. 8b (i.e., the transition from a F_p-$WSOC_p$ dependence to no dependence).

The differences between the F_p-OC and F_p-$WSOC_p$ relationships may be due to composition differences between the two systems and may at the very least suggest that the chemical nature of the absorbing organic phase is a meaningful parameter to the partitioning process. Seinfeld et al. (2001) found a similar effect with water uptake in modeling studies; partitioning of hydrophilic compounds to the particle phase was enhanced by particulate water uptake while that for hydrophobic compounds was diminished by water uptake. Our results are also in general agreement with that of Bowman and Karamalegos (2002), who found a compositional effect on SOA mass concentrations in model simulations based on the affinity between partitioning SVOCs

and the absorbing organic phase (i.e., due to the effect of the composition-dependent activity coefficient, ζ, on K_p). In a heterogeneous SOA formation chamber experiment, Volkamer et al. (2008) found a relationship between the gas/particle partitioning of C_2H_2-OH products (e.g., glyoxal) and the existing organic aerosol composition.

It is noteworthy that the differences in F_p verse $WSOC_p$ and OC were present despite an observed high correlation between $WSOC_p$ and OC (R^2=0.73, see above), and despite $WSOC_p$ accounting for, on average, 70% of OC. This implies that approximately 30% of OC was insoluble in water, and similarities between this water-insoluble organic carbon fraction and the EC diurnal profiles suggest that these insoluble organic compounds (calculated as OC-$WSOC_p$) were largely primary (Fig. 3). These primary compounds are chemically much different from $WSOC_p$, including significant differences in oxidation, functional groups, and polarity (Saxena and Hildemann, 1996). The primary component of OC, and its different chemical character from that of WSOC, may in part explain the lack of an F_p dependence on OC. Though the general trends in data and fit in Fig. 8b are somewhat similar to the smog chamber SOA Yield-M_o relationship found by Odum et al. (1996), where in that case M_o was OC mass formed in the chamber, it is also possible that the F_p-$WSOC_p$ relationship results from a completely different process than absorptive partitioning. A difference between the ambient F_p-$WSOC_p$ trend and that of the chamber Yield-OM is that the F_p-$WSOC_p$ dependence appears to end at some point, whereas the Yield-OM dependence for chamber data shows a continuing positive OM effect. Additionally, the results in Fig. 9a and b suggest that RH and $WSOC_p$ impact WSOC partitioning through different means. The high RH analysis in Fig. 9b only included data with RH levels above 65% (mean RH=78.2%) while the low RH analysis only included data with RH levels below 50% (mean RH=38.5%). This contrasts how $WSOC_p$ affects partitioning for very wet versus very dry particles.

The results in Fig. 9a and b indicate that the process is similar on wet and dry particles. This has two implications. First, the role that the particle organic component (e.g., $WSOC_p$) plays in partitioning is present even when particle H_2O concentrations likely far exceeded $WSOC_p$ concentrations. This behavior would not be expected if partition-

ing were described solely by the partitioning coefficient, K_p. As the liquid water content of particles increases, the importance of water in the partitioning process should increase and the importance of the $WSOC_p$ concentration should diminish. This is due to the significant impact of water on the average molecular weight of the absorbing organic plus aqueous phase, MW_{om}, and on the increase it would bring to the total mass of the absorbing organic plus aqueous phase, M_o (Eq. 3). For example, at RH levels above 90%, the liquid water concentration may be an order of magnitude higher than the $WSOC_p$ concentration, and so would dictate any relationship with M_o. Our ambient results suggest that this did not occur with WSOC partitioning: at the highest RH levels, the $WSOC_p$ concentration still appears to be important (Fig. 9a and b). It indicates that $WSOC_p$ and liquid water both somewhat independently contribute to WSOC gas/particle partitioning. As an example, the liquid water may affect absorption of the water-soluble gases, and the $WSOC_p$ in the particle may influence the heterogeneous production of lower vapor pressure products. The types of heterogeneous reactions that take place in the liquid particle may account for the observed F_p dependence on $WSOC_p$. Secondly, because the curve for the much dryer particles (Fig. 9b) is essentially identical in shape to the wet particles, the overall partitioning mechanism appears to be similar throughout the RH range measured: the role of water is not just confined to RH>80% when particles rapidly absorb water and are very wet.

There is substantial evidence from both laboratory and ambient studies suggesting that heterogeneous chemical reactions are important. Limbeck et al. (2003) observed a significant increase in isoprene SOA yields in the presence of acidic seed particles compared with yields in the presence of neutral seed particles in smog chamber studies. Kroll et al. (2007) found systematically higher experimental SOA yields from aromatic VOCs in the presence of ammonium sulfate seed particles compared to experiments in which no seed particles were present. In experiments designed to simulate the chemistry occurring within cloud droplets, Altieri et al. (2008) observed the formation of oligomers from methylglyoxal. Volkamer et al. (2008) observed SOA formation from acetylene in smog chamber experiments and attributed this to the formation of

glyoxal and its subsequent uptake and reaction in particles. The results of Volkamer et al. (2008) included a linear correlation between SOA yields and aerosol liquid water concentrations, and an apparent effect of the existing organic aerosol composition on SOA yields as well, very similar to our findings. These represent a small sampling of experimental studies in which heterogeneous reactions were observed. There have been numerous ambient studies which have identified macromolecular organic compounds, or oligomers, as components of organic aerosol (e.g., Kalberer et al., 2006; Denkenberger et al., 2007). It is highly unlikely that oligomer formation occurs strictly through gas-phase processes, thus their presence in ambient particles confirms the occurrence of particle-phase reactions as well.

3.3 General discussions/implications

Since the above findings are based on extensive measurements in the ambient atmosphere, they have significant relevance for both regulatory and modeling applications. First, the observed NO_x effect on F_p could have links to control strategies of O_3 and $PM_{2.5}$, criteria pollutants which annually exceed EPA attainment limits in Atlanta (http://www.epa.gov/oar/oaqps/greenbk/). At high NO_x levels, F_p values were lower compared to those at low NO_x levels, indicating that a higher fraction of the total WSOC was in the particle phase when NO_x levels were low. This was attributed to the influence NO_x imparts on the product distribution in VOC oxidation. Atlanta is a NO_x-limited environment, which suggests NO_x reductions may be the most effective means of controlling O_3 concentrations. The present results indicate that mitigating O_3 concentrations through NO_x reductions could produce the unwanted effect of an increase in $PM_{2.5}$ mass concentrations. This potential feedback to NO_x control is noteworthy and should be examined in more detail. There is evidence, however, that some other anthropogenic component may also influence $WSOC_p$ production, signifying that there may be additional unidentified processes leading to SOA formation that could still restrict accurate prediction (Weber et al., 2007; Hennigan et al., 2008b).

The combined findings presented in this paper make a strong case that the tradi-

tional SOA theory based solely on the K_p formulation (Eq. 3) is not a suitable predictor of SOA in Atlanta. SOA partitioning theory predicts a strong relationship between K_p (i.e., F_p) and OC (e.g., Odum et al., 1996) that was not seen in our ambient data. A relationship was observed between F_p and $WSOC_p$, though it differed from the relationships observed in chamber studies. K_p theory predicts a strong effect of water on partitioning, and a strong F_p-RH effect was seen in the ambient results. However, K_p theory also predicts that as H_2O is increased to levels significantly higher than $WSOC_p$ (or OC), the importance of $WSOC_p$ in the partitioning process should be diminished. This phenomenon was not observed in the ambient data, where the $WSOC_p$ concentration remained an important factor for WSOC gas/particle partitioning even at the highest RH levels. A mechanism that incorporates both a partitioning of SVOCs to fine particle water and the reaction of organic compounds in the aqueous phase may better represent the partitioning that occurs in the Atlanta summer.

Further ambient studies are required to investigate whether or not the findings presented here are similar in other locations. Additional studies are also needed to provide insight into the specific SVOCs that are involved and to identify possible heterogeneous chemical mechanisms that may be prominent in ambient SOA formation.

4 Conclusions

Overall, the present results provide a detailed characterization of SOA partitioning in the summertime in Atlanta, a large urban center with substantial biogenic VOC emissions. Partitioning, analyzed through the fraction of total WSOC in the particle phase, F_p, was found to have no dependence on temperature, though this was likely due to the emissions of precursor VOCs and the formation of WSOC (in the gas and particle phase), which both could have temperature dependences. F_p was related to NO_x concentrations, with higher NO_x levels corresponding to lower values of F_p. Although not likely related to the partitioning process, it could be attributed to the effect of NO_x on the product distribution in VOC oxidation. In previous work, F_p was shown to have

a very strong dependence on relative humidity at RH levels above 70% due to the uptake of liquid water by fine particles. The current work also shows a strong partitioning dependence on the existing $WSOC_p$ concentration, but not on the OC concentration, possibly indicating that either chemical similarity between partitioning SVOCs and the absorbing aerosol phase is important, or the role of heterogeneous chemistry in SOA formation. The relationship between F_p and $WSOC_p$ was present even at the highest RH levels, when the liquid water concentration was likely far greater than the $WSOC_p$ concentration. Collectively, the results point to liquid-phase heterogeneous chemical reactions as a major SOA formation process and are remarkably similar to the recent chamber experiments of Volkamer et al. (2008).

Finally, the summertime data indicate that $WSOC_p$ incorporated most, if not all, of the SOA in Atlanta. To our knowledge, this represents the first detailed characterization of SOA formation processes based on ambient data. Previous studies have described the gas/particle partitioning of the total SOA within a smog chamber, and previous ambient studies have reported on the partitioning of individual compounds. The results provide important insight into SOA formation and the gas/particle partitioning process beyond the current scientific understanding. Specifically, that fine-particle water and heterogeneous chemical reactions may be a significant, and possibly the single most important mechanism for SOA formation in summertime Atlanta. This mechanism may also play an important role in other locations (e.g., Hennigan et al., 2008c), and may explain the systematic under-prediction of SOA by most models.

Acknowledgement. R. Weber thanks the National Science Foundation for their financial support through grant ATM-0802237. The generous financial gift from F. Cullen and L. Peck also made this work possible.

References

Altieri, K. E., Seitzinger, S. P., Carlton, A. G., Turpin, B. J., Klein, G. C., and Marshall, A. G.: Oligomers formed through in-cloud methylglyoxal reactions: Chemical composition, proper-

ties, and mechanisms investigated by ultra-high resolution FT-ICR mass spectrometry, Atmos. Environ., 42(7), 1476–1490, 2008.
Anderson, C. H., Dibb, J. E., Griffin, R. J., Hagler, G. S. W., and Bergin, M. H.: Atmospheric water-soluble organic carbon measurements at Summit, Greenland, Atmos. Environ., 42(22), 5612–5621, doi:10.1016/j.atmosenv.2008.03.06, 2008.
Bowman, F. M. and Karamalegos, A. M.: Estimated effects of composition on secondary organic aerosol mass concentrations, Environ. Sci. Technol., 36(12), 2701–2707, 2002.
Chang, E. I. and Pankow, J. F.: Organic particulate matter formation at varying relative humidity using surrogate secondary and primary organic compounds with activity corrections in the condensed phase obtained using a method based on the Wilson equation, Atmos. Chem. Phys. Discuss., 8, 995–1039, 2008, http://www.atmos-chem-phys-discuss.net/8/995/2008/.
Chu, S.-H., Paisie, J. W., and Jang, B. W.-L.: PM data analysis – a comparison of two urban areas: Fresno and Atlanta, Atmos. Environ., 38, 3155–3164, 2004.
Cocker, D. R., Clegg, S. L., Flagan, R. C., and Seinfeld, J. H.: The effect of water on gas-particle partitioning of secondary organic aerosol. Part 1: α-pinene/ozone system, Atmos. Environ., 35(35), 6049–6072, 2001a.
Cocker, D. R., Mader, B. T., Kalberer, M., Flagan, R. C., and Seinfeld, J. H.: The effect of water on gas-particle partitioning of secondary organic aerosol: Part 2: m-xylene and 1,3,5-trimethylbenzene photooxidation systems, Atmos. Environ., 35(35), 6073–6085, 2001b.
Cofer, W. R. and Edahl, R. A.: A new technique for collection, concentration and determination of gaseous tropospheric formaldehyde, Atmos. Environ., 20(5), 979–984, 1986.
Cornbleet, P. J. and Gochman, N.: Incorrect least-squares regression coefficients in method-comparison analysis, Clin. Chem., 25, 432–438, 1979.
de Gouw, J. A., Middlebrook, A. M., Warneke, C., Goldan, P. D., Kuster, W. C., Roberts, J. M., Fehsenfeld, F. C., Worsnop, D. R., Canagaratna, M. R., Pszenny, A. A. P., Keene, W. C., Marchewka, M., Bertman, S. B., and Bates, T. S.: Budget of organic carbon in a polluted atmosphere: results from the New England Air Quality Study in 2002, J. Geophys. Res.-Atmos., 110, D16305, doi:10.1029/2004JD005623, 2005.
Denkenberger, K. A., Moffet, R. C., Holecek, J. C., Rebotier, T. P., and Prather, K. A.: Real-time, single-particle measurements of oligomers in aged ambient aerosol particles, Environ. Sci. Technol., 41(15), 5439–5446, 2007.
Edney, E. O., Driscoll, D. J., Speer, R. E., Weathers, W. S., Kleindienst, T. E., Li, W., and Smith, D. F.: Impact of aerosol liquid water on secondary organic aerosol yields of irradi-

ated toluene/propylene/NO_x/$(NH_4)(2)$ SO_4/air mixtures, Atmos. Environ., 34(23), 3907–3919, 2000.
Environmental Protection Agency, National Emissions Inventory: www.epa.gov/ttn/chief/net/2002inventory.html, 2008.
Ervens, B., Carlton, A. G., Turpin, B. J., Altieri, K. E., Kreidenweis, S. M., and Feingold, G.: Secondary organic aerosol yields from cloud-processing of isoprene oxidation products, Geophys. Res. Lett., 35, L02816, doi:10.1029/2007GL031828, 2008.
Favez, O., Sciare, J., Cachier, H., Alfaro, S. C., and Abdelwahab, M. M.: Significant formation of water-insoluble secondary organic aerosols in semi-arid urban environment, Geophys. Res. Lett., 35, L15801, doi:10.1029/2008GL034446, 2008.
Fisseha, R., Dommen, J., Gaeggeler, K., Weingartner, E., Samburova, V., Kalberer, M., and Baltensperger, U.: Online gas and aerosol measurement of water soluble carboxylic acids in Zurich, J. Geophys. Res.-Atmos., 111, D12316, doi:10.1029/2005JD006782, 2006.
Georgia Department of Natural Resources Ambient Monitoring Network (http://www.georgiaepd.org/air/amp/), 2008.
Goldstein, A. H. and Galbally, I. E.: Known and unexplored organic constituents in the earth's atmosphere, Environ. Sci. Technol., 41(5), 1514–1521, 2007.
Griffin, R. J., Cocker, D. R., Flagan, R. C., and Seinfeld, J. H.: Organic aerosol formation from the oxidation of biogenic hydrocarbons, J. Geophys. Res.-Atmos., 104(D3), 3555–3567, 1999.
Guenther, A., Zimmerman, P., and Wildermuth, M.: Natural volatile organic compound emission rate estimates for United States woodland landscapes, Atmos. Environ., 28(6), 1197–1210, 1994.
Hakola, H., Laurila, T., Rinne, J., and Puhto, K.: The ambient concentrations of biogenic hydrocarbons at a northern European, boreal site, Atmos. Environ., 34(29–30), 4971–4982, 2000.
Hallquist, M., Wangberg, I., Ljungstrom, E., Barnes, I., and Becker, K. H.: Aerosol and product yields from NO_3 radical-initiated oxidation of selected monoterpenes, Environ. Sci. Technol., 33(4), 553–559, 1999.
Hennigan, C. J., Bergin, M. H., Dibb, J. E., and Weber, R. J.: Enhanced secondary organic aerosol formation due to water uptake by fine particles, Geophys. Res. Lett., 35, L18801, doi:10.1029/2008GL035046, 2008a.
Hennigan, C. J., Bergin, M. H., and Weber, R. J.: Correlations between water-soluble organic

aerosol and water vapor: A synergistic effect from biogenic emissions?, Environ. Sci. Technol., 42(24), 9079–9085, 2008b.
Hennigan, C. J., Sullivan, A. P., Fountoukis, C. I., Nenes, A., Hecobian, A., Vargas, O., Hanks, A. T. C., Huey, L. G., Lefer, B. L., Russell, A. G., and Weber, R. J.: On the volatility and production mechanisms of newly formed nitrate and water soluble organic aerosol in Mexico City, Atmos. Chem. Phys., 8, 3761–3768, 2008c, http://www.atmos-chem-phys.net/8/3761/2008/.
Hoffmann, T., Odum, J. R., Bowman, F., Collins, D., Klockow, D., Flagan, R. C., and Seinfeld, J. H.: Xb, formation of organic aerosols from the oxidation of biogenic hydrocarbons, J. Atmos. Chem., 26(2), 189–222, 1997.
Jang, M. S. and Kamens, R. M.: Atmospheric secondary aerosol formation by heterogeneous reactions of aldehydes in the presence of a sulfuric acid aerosol catalyst, Environ. Sci. Technol., 35(24), 4758–4766, 2001.
Janson, R., Rosman, K., Karlsson, A., and Hansson, H. C.: Biogenic emissions and gaseous precursors to forest aerosols, Tellus B, 53(4), 423–440, 2001.
Kalberer, M., Sax, M., and Samburova, V.: Molecular size evolution of oligomers in organic aerosols collected in urban atmospheres and generated in a smog chamber, Environ. Sci. Technol., 40(19), 5917–5922, 2006.
Kroll, J. H. and Seinfeld, J. H.: Chemistry of secondary organic aerosol: formation and evolution of low-volatility organics in the atmosphere, Atmos. Environ., 42(16), 3593–3624, 2008.
Kroll, J. H., Chan, A. W. H., Ng, N. L., Flagan, R. C., and Seinfeld, J. H.: Reactions of semivolatile organics and their effects on secondary organic aerosol formation, Environ. Sci. Technol., 41(10), 3545–3550, 2007.
Kroll, J. H., Ng, N. L., Murphy, S. M., Flagan, R. C., and Seinfeld, J. H.: Secondary organic aerosol formation from isoprene photooxidation, Environ. Sci. Technol., 40(6), 1869–1877, 2006.
Liggio, J., Li, S. M., and McLaren, R.: Reactive uptake of glyoxal by particulate matter, J. Geophys. Res.-Atmos., 110(D10), 13, 2005.
Limbeck, A., Kulmala, M., and Puxbaum, H.: Secondary organic aerosol formation in the atmosphere via heterogeneous reaction of gaseous isoprene on acidic particles, Geophys. Res. Lett., 30(19), 4, 2003.
Malm, W. C. and Day, D. E.: Estimates of aerosol species scattering characteristics as a function of relative humidity, Atmos. Environ., 35(16), 2845–2860, 2001.

Marple, V. A., Rubow, K. L., and Behm, S. M.: A microorifice uniform deposit impactor (MOUDI) – description, calibration, and use, Aerosol Sci. Tech., 14(4), 434–446, 1991.
Matsunaga, S. N., Kato, S., Yoshino, A., Greenberg, J. P., Kajii, Y., and Guenther, A. B.: Gas-aerosol partitioning of semi volatile carbonyls in polluted atmosphere in Hachioji, Tokyo, Geophys. Res. Lett., 32, L11805, doi:10.1029/2004GL021893, 2005.
Miyazaki, Y., Kondo, Y., Takegawa, N., Komazaki, Y., Fukuda, M., Kawamura, K., Mochida, M., Okuzawa, K., and Weber, R. J.: Time-resolved measurements of water-soluble organic carbon in Tokyo, J. Geophys. Res.-Atmos., 111, D23206, 12, doi:10.1029/2006JD007125, 2006.
Ng, N. L., Kroll, J. H., Chan, A. W. H., Chhabra, P. S., Flagan, R. C., and Seinfeld, J. H.: Secondary organic aerosol formation from *m*-xylene, toluene, and benzene, Atmos. Chem. Phys., 7, 3909–3922, 2007, http://www.atmos-chem-phys.net/7/3909/2007/.
NIOSH: Elemental Carbon (Diesel Particulate): Method 5040, in: NIOSH Manual of Analytical Methods, edited by: Eller, P. M. and Cassinelli, M. E., National Institute for Occupational Safety and Health, Cincinnati, 1996.
Odum, J. R., Jungkamp, T. P. W., Griffin, R. J., Flagan, R. C., and Seinfeld, J. H.: The atmospheric aerosol-forming potential of whole gasoline vapor, Science, 276(5309), 96–99, 1997.
Odum, J. R., Hoffmann, T., Bowman, F., Collins, D., Flagan, R. C., and Seinfeld, J. H.: Va, gas/particle partitioning and secondary organic aerosol yields, Environ. Sci. Technol., 30(8), 2580–2585, 1996.
Orsini, D. A., Ma, Y. L., Sullivan, A., Sierau, B., Baumann, K., and Weber, R. J.: Refinements to the particle-into-liquid sampler (PILS) for ground and airborne measurements of water soluble aerosol composition, Atmos. Environ., 37(9–10), 1243–1259, 2003.
Pandis, S. N., Paulson, S. E., Seinfeld, J. H., and Flagan, R. C.: Aerosol formation in the photooxidation of isoprene and β-pinene, Atmos. Environ. A-Gen., 25(5–6), 997–1008, 1991.
Pankow, J. F.: An absorption model of the gas aerosol partitioning involved in the formation of secondary organic aerosol, Atmos. Environ., 28(2), 189–193, 1994.
Pankow, J. F. and Bidleman, T. F.: Effects of temperature, TSP and percent nonexchangeable material in determining the gas particle partitioning of organic compounds, Atmos. Environ. A-Gen., 25(10), 2241–2249, 1991.
Peltier, R. E., Weber, R. J., and Sullivan, A. P.: Investigating a liquid-based method for online organic carbon detection in atmospheric particles, Aerosol Sci. Technol., 41(12), 1117–1127,

2007.
Presto, A. A., Hartz, K. E. H., and Donahue, N. M.: Secondary organic aerosol production from terpene ozonolysis. 2. Effect of NO_x concentration, Environ. Sci. Technol., 39(18), 7046–7054, 2005.
Pun, B. K. and Seigneur, C.: Investigative modeling of new pathways for secondary organic aerosol formation, Atmos. Chem. Phys., 7, 2199–2216, 2007, http://www.atmos-chem-phys.net/7/2199/2007/.
Sander, R.: Compilation of Henry's Law Constants for Inorganic and Organic Species of Potential Importance in Environmental Chemistry, Version 3, http://www.mpch-mainz.mpg.de/~sander/res/henry.html, 1999.
Saxena, P. and Hildemann, L. M.: Un, Water-soluble organics in atmospheric particles: A critical review of the literature and application of thermodynamics to identify candidate compounds, J. Atmos. Chem., 24(1), 57–109, 1996.
Seinfeld, J. H., Erdakos, G. B., Asher, W. E., and Pankow, J. F.: Modeling the formation of secondary organic aerosol (SOA). 2. The predicted effects of relative humidity on aerosol formation in the α-pinene-, β-pinene-, sabinene-, Delta(1)-Carene-, and cyclohexene-ozone systems, Environ. Sci. Technol., 35(9), 1806–1817, 2001.
Seinfeld, J. H. and Pandis, S. N.: Atmospheric Chemistry and Physics, from Air Pollution to Climate Change, John Wiley & Sons, New York, NY, 1998.
Simon, V., Clement, B., Riba, M. L., and Torres, L.: The LANDES experiment – Monoterpenes emitted from the maritime pine, J. Geophys. Res.-Atmos., 99(D8), 16501–16510, 1994.
Spaulding, R. S., Talbot, R. W., and Charles, M. J.: Optimization of a mist chamber (cofer scrubber) for sampling water-soluble organics in air, Environ. Sci. Technol., 36(8), 1798–1808, 2002.
Sullivan, A. P., Peltier, R. E., Brock, C. A., de Gouw, J. A., Holloway, J. S., Warneke, C., Wollny, A. G., and Weber, R. J.: Airborne measurements of carbonaceous aerosol soluble in water over northeastern United States: method development and an investigation into water-soluble organic carbon sources, J. Geophys. Res.-Atmos., 111, D23S46, doi:10.1029/2006JD007072, 2006.
Sullivan, A. and Weber, R. J.: Chemical characterization of the ambient organic aerosol soluble in water Part 2: Isolation of acid, neutral, and basic fractions by modified size exclusion chromatography, J. Geophys. Res., 111(D5), D05315, doi:10.1029/2005JD006486, 2006.
Sullivan, A. P., Weber, R. J., Clements, A. L., Turner, J. R., Bae, M. S., and

Schauer, J. J.: A method for on-line measurement of water-soluble organic carbon in ambient aerosol particles: results from an urban site, Geophys. Res. Lett., 31, L13105, doi:10.1029/2004GL019681, 2004.

Takekawa, H., Minoura, H., and Yamazaki, S.: Temperature dependence of secondary organic aerosol formation by photo-oxidation of hydrocarbons, Atmos. Environ., 37(24), 3413–3424, 2003.

Tingey, D. T., Manning, M., Grothaus, L. C., and Burns, W. F.: Influence of light and temperature on monoterpene emission rates from slash pine, Plant Physiol., 65(5), 797–801, 1980.

Tsigaridis, K., Lathière, J., Kanakidou, M., and Hauglustaine, D. A.: Naturally driven variability in the global secondary organic aerosol over a decade, Atmos. Chem. Phys., 5, 1891–1904, 2005, http://www.atmos-chem-phys.net/5/1891/2005/.

Volkamer, R., Ziemann, P. J., and Molina, M. J.: Secondary organic aerosol formation from acetylene (C_2H_2): seed effect on SOA yields due to organic photochemistry in the aerosol aqueous phase, Atmos. Chem. Phys. Discuss., 8, 14841–14892, 2008, http://www.atmos-chem-phys-discuss.net/8/14841/2008/.

Weber, R. J., Sullivan, A. P., Peltier, R. E., Russell, A., Yan, B., Zheng, M., de Gouw, J., Warneke, C., Brock, C., Holloway, J. S., Atlas, E. L., and Edgerton, E.: A study of secondary organic aerosol formation in the anthropogenic-influenced southeastern United States, J. Geophys. Res.-Atmos., 112, D13302, doi:10.1029/2007JD008408, 2007.

Weber, R., Orsini, D., Bergin, M., Kiang, C. S., Chang, M., John, J. S., Carrico, C. M., Lee, Y. N., Dasgupta, P., Slanina, J., Turpin, B., Edgerton, E., Hering, S., Allen, G., Solomon, P., and Chameides, W.: Short-term temporal variation in $PM_{2.5}$ mass and chemical composition during the Atlanta supersite experiment, 1999, J. Air Waste Manage., 53(1), 84–91, 2003.

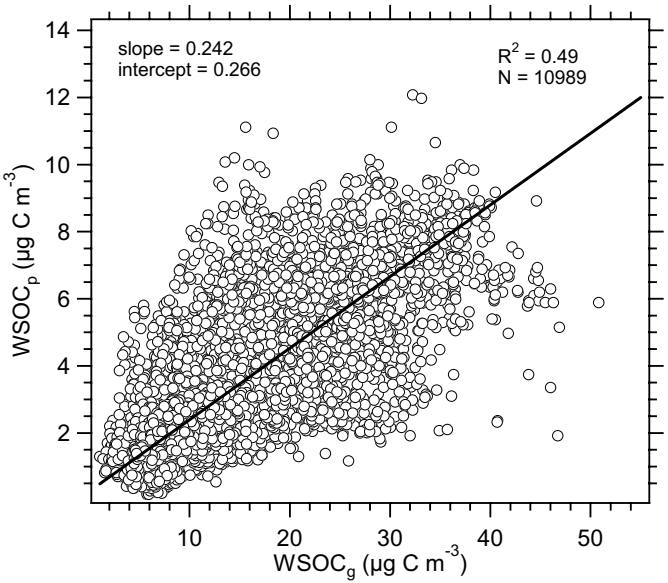

Fig. 1. Scatter plot of $WSOC_p$ verse $WSOC_g$ for the entire summer data set.

ACPD
9, 635–671, 2009

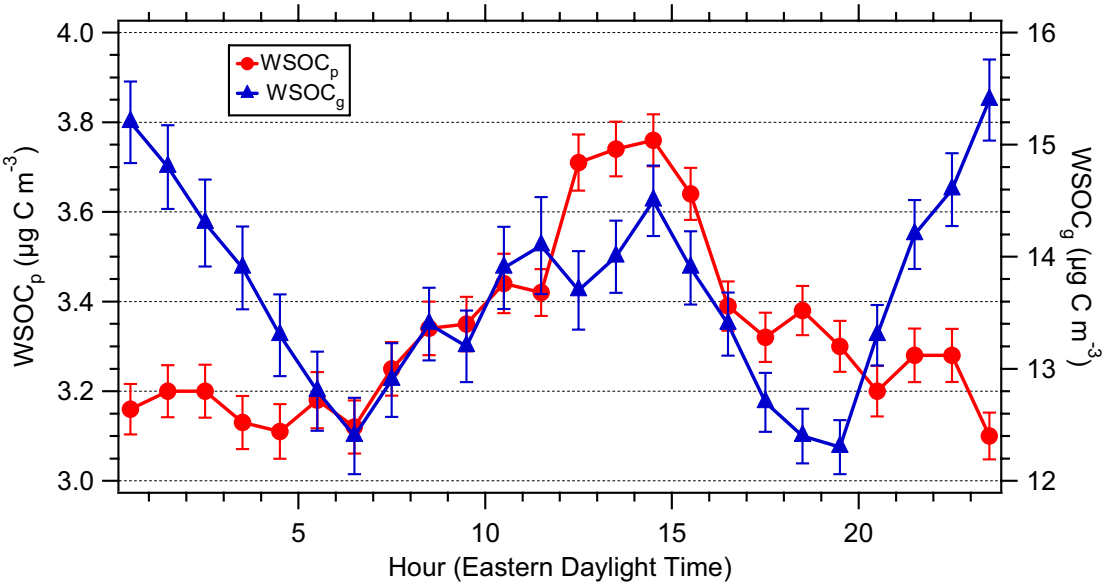

Fig. 2. Average diurnal profiles for WSOC$_p$ and WSOC$_g$. The vertical bars on each data point represent the standard error (standard deviation/$\sqrt{}$N). Eastern daylight time is local time, and is Eastern Standard Time plus one hour.

ACPD
9, 635–671, 2009

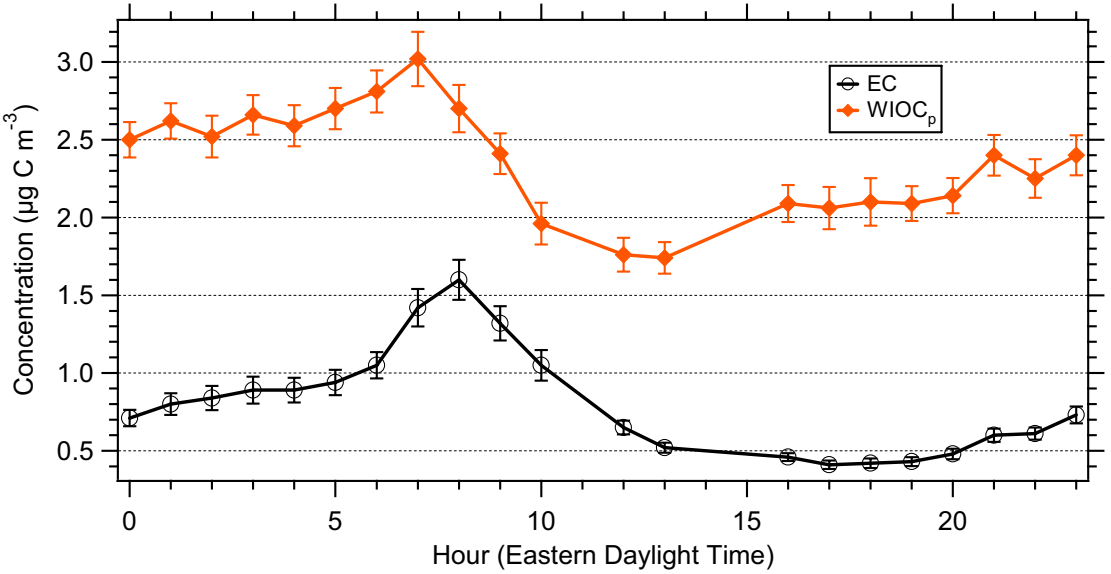

Fig. 3. Average diurnal profiles of EC and Water-Insoluble Organic Carbon (WIOC$_p$). WIOC$_p$ was not measured directly, but was calculated as OC–WSOC$_p$. The vertical bars on each data point represent the standard error (standard deviation/$\sqrt{}$N).

ACPD
9, 635–671, 2009

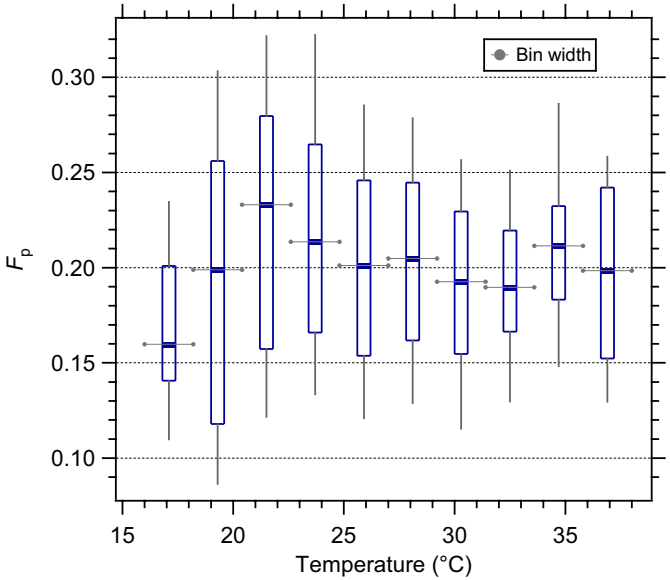

Fig. 4. Box plot of particulate WSOC fraction, F_p, verse Temperature. The box plot was generated by segregating the data into ten equally-spaced temperature bins (average N per bin=1040), and median values (thick horizontal bar), 25th and 75th percentiles (lower and upper box bounds, respectively), and 10th and 90th percentiles (lower and upper whiskers, respectively) for each bin are plotted.

ACPD
9, 635–671, 2009

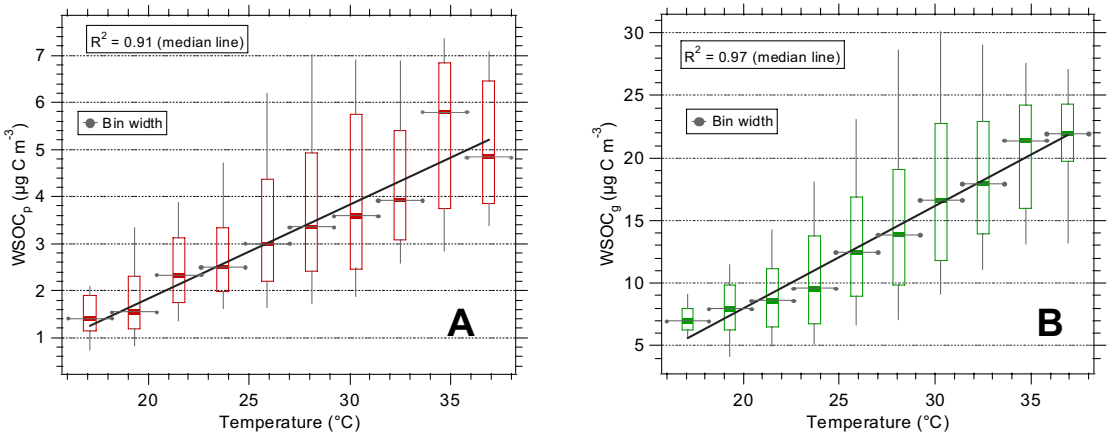

Fig. 5. Box plots of $WSOC_p$ **(a)** and $WSOC_g$ **(b)** verse Temperature. The plots show median values (thick horizontal bar), 25th and 75th percentiles (lower and upper box bounds, respectively), and 10th and 90th percentiles (lower and upper whiskers, respectively) for each bin. For the $WSOC_p$–T plot (a), the average N per bin=1803, and for the $WSOC_g$–T plot, the average N per bin=1165.

ACPD
9, 635–671, 2009

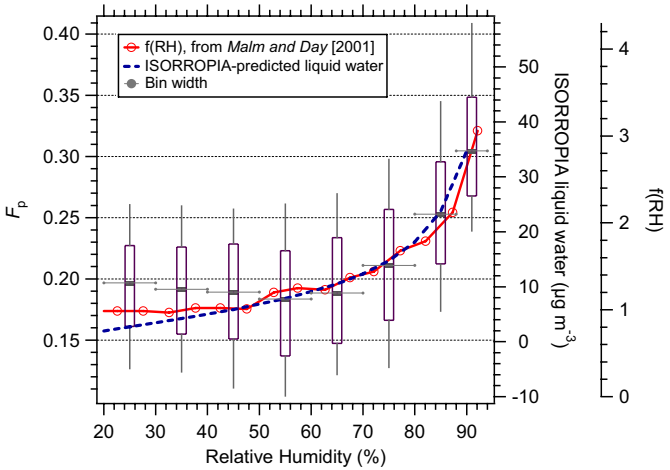

Fig. 6. Relationship between partitioning and liquid water uptake, adapted from Hennigan et al. (2008). The box and whiskers represent ambient F_p data, with median values (thick horizontal bar), 25th and 75th percentiles (lower and upper box bounds, respectively), and 10th and 90th percentiles (lower and upper whiskers, respectively) shown for each bin. ISORROPIA-predicted liquid water as a function of RH is based on an average inorganic aerosol composition, and the f(RH) trace is a measure of the scattering enhancement due to particulate water uptake reported by Malm and Day (2001).

ACPD
9, 635–671, 2009

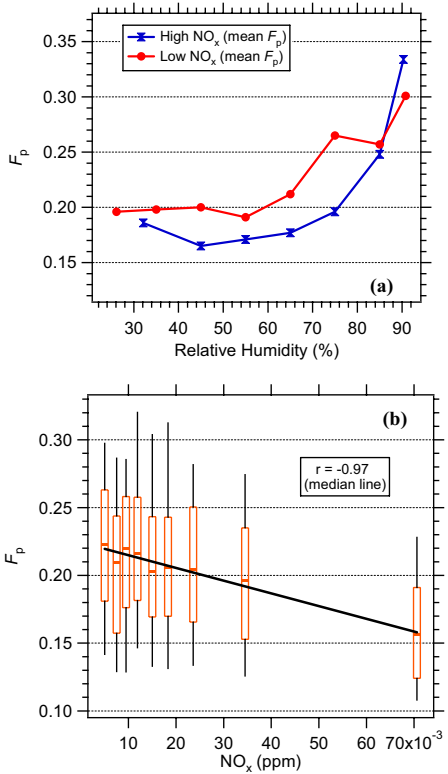

Fig. 7. Relationship between NO_x and F_p. Mean F_p verse RH for data sorted by NO_x concentration **(a)** (Data represent the highest and lowest 35% of NO_x concentrations). Particulate WSOC fraction, F_p, as a function of NO_x concentrations **(b)**. The data were binned according to NO_x concentrations and median (thick horizontal line), 25th and 75th percentiles (lower and upper box), and 10th and 90th percentiles (lower and upper whiskers) are shown for each bin (average N per bin=197).

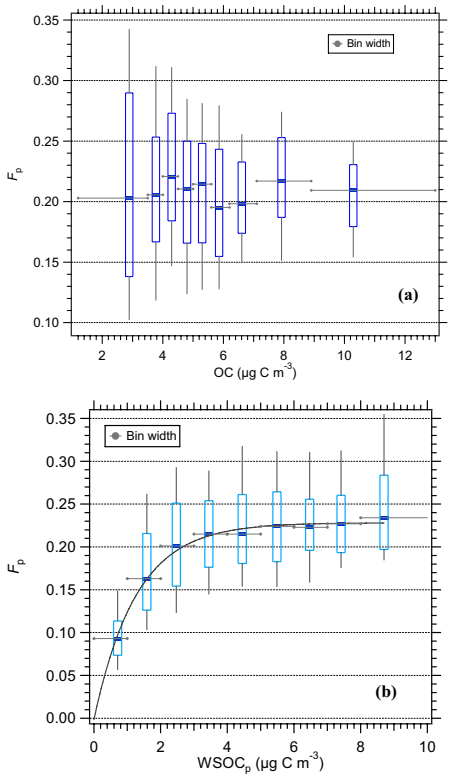

Fig. 8. WSOC partitioning (F_p) as a function of OC concentration **(a)** and WSOC$_p$ concentration **(b)**. For the box plot of particulate WSOC fraction, F_p, verse OC **(a)**, which shows median values (thick horizontal bar), 25th and 75th percentiles (lower and upper box bounds, respectively), and 10th and 90th percentiles (lower and upper whiskers, respectively) for each bin, average N per bin=139. For the box plot of F_p verse WSOC$_p$ **(b)**, average N per bin=1220. The curve is forced through zero based on the definition of F_p (Eq. 1).

ACPD
9, 635–671, 2009

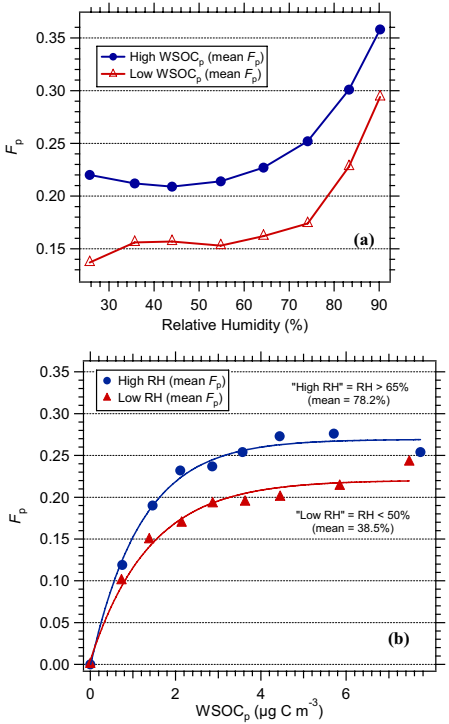

Fig. 9. WSOC partitioning as a function of RH and WSOC$_p$ concentration. Mean F_p values verse RH for the highest (mean WSOC$_p$=5.3 µg C m^{-3}) and lowest (mean WSOC$_p$=1.7 µg C m^{-3}) 35% of WSOC$_p$ concentrations **(a)**. Mean F_p values as a function WSOC$_p$, segregated for high and low RH levels **(b)**. The two data points at (0, 0) are not measured, but are based on the definition of F_p (Eq. 1). Note that the curves only represent the central tendency and that there is considerable scatter about the mean (e.g., see Fig. 8b).